molecular pharmaceutics

articles

Synthesis of Oligo(ethylenediamino)-β-Cyclodextrin Modified Gold Nanoparticle as a DNA Concentrator

Hao Wang, Yong Chen, Xiao-Yun Li, and Yu Liu*

Department of Chemistry, State Key Laboratory of Elemento-Organic Chemistry, Nankai University, Tianjin 300071, P. R. China

Received April 18, 2006; Revised Manuscript Received December 7, 2006; Accepted December 13, 2006

Abstract: A novel oligo(ethylenediamino)-β-cyclodextrin-modified gold nanoparticle (OEA-CD-NP) was synthesized as a vector for DNA binding and comprehensively investigated by means of absorption and circular dichroism spectroscopies as well as transmission electron microscopy, and its plasmid transfection efficiency as a carrier into cultivated cells *in vitro* was also evaluated. Possessing many hydrophobic cavities at the outer space, OEA-CD-NP may have a capability of carrying biological and/or medicinal substrates into cells, which will make it potentially applicable in many fields of material science and biological technology. In contrast with OEA-CD-NP, the oligo(ethylenediamino)-lipoic amido-modified gold nanoparticle (OEA-L-NP) without CD was synthesized to investigate the interaction with DNA. The results showed that OEA-L-NPs could only weakly bind DNA.

Keywords: Nanoparticles; cyclodextrin; DNA; gene transfection; cytotoxicity

Introduction

Notably, several kinds of biomaterials for gene delivery, e.g., collagen,[1] polymers,[2] cationic liposomes,[3] oligopeptides,[4] poly(L-lysine),[5] polyethylenimine,[6,7] and dendrimers,[8] have been developed to condense DNA and achieve the localized and sustained delivery of genes. In recent years, surface-modified silica nanoparticles[9] and monolayer-protected gold nanoparticles[10] were reported to be able to successfully act

* Author to whom correspondence should be addressed. Mailing address: Department of Chemistry, State Key Laboratory of Elemento-Organic Chemistry, Nankai University, Tianjin 300071, P. R. China. Tel: +86-22-23503625. Fax: +86-22-23503625. E-mail: yuliu@nankai.edu.cn.

(1) (a) Fang, J.; Zhu, Y. Y.; Smiley, E.; Bonadio, J.; Rouleau, J. P.; Goldstein, S. A.; McCauley, L. K.; Davidson, B. L.; Roessler, B. J. Stimulation of new bone formation by direct transfer of osteogenic plasmid genes. *Proc. Natl. Acad. Sci. U.S.A.* **1996**, *93*, 5753−5758. (b) Scherer, F.; Schillinger, U.; Putz, U.; Stemberger, A.; Plank, C. Nonviral vector loaded collagen sponges for sustained gene delivery in vitro and in vivo. *J. Gene Med.* **2002**, *4*, 634−643.

(2) (a) Li, Z.; Ning, W.; Wang, J.; Choi, A.; Lee, P. Y.; Tyagi, P.; Huang, L. Controlled gene delivery system based on thermosensitive biodegradable hydrogel. *Pharm. Res.* **2003**, *20*, 884−888. (b) Hoffman, A. S. Hydrogels for biomedical applications. *Adv. Drug Delivery Rev.* **2002**, *54*, 3−12. (c) Hennink, W. E.; van Nostrum, C. F. Novel crosslinking methods to design hydrogels *Adv. Drug Delivery Rev.* **2002**, *54*, 13−36.

(3) Coeytaux, E.; Coulaud, D.; Cam, E. L.; Danos, O.; Kichler, A. The cationic amphipathic α-helix of HIV-1 viral protein r(vpr) binds to nucleic acids. *J. Biol. Chem.* **2003**, *278*, 18110−18116.

(4) Morris, M. C.; Chaloin, L.; Heitz, F.; Divita, G. Translocating peptides and proteins and their use for gene delivery. *Curr. Opin. Biotechnol.* **2000**, *11*, 461−466.

(5) Perales, J. C.; Ferkol, T.; Molas, M.; Hanson, R. W. An evaluation of receptor-mediated gene transfer using synthetic DNA-ligand complexes. *Eur. J. Biochem.* **1994**, *226*, 255−266.

(6) Coll, J. L.; Chollet, P.; Brambilla, E.; Desplanques, D.; Behr, J. P.; Favrot, M. In vivo delivery to tumors of DNA complexed with linear polyethylenimine. *Hum. Gene Ther.* **1999**, *10*, 1659−1666.

(7) (a) Boussif, O.; Lezoualc'h, F.; Zanta, A.; Mergny, M. D.; Scherman, D.; Demeneix, B.; Behr, J.-P. A versatile vector for gene and oligonucleotide transfer into cells in culture and in vivo: polyethylenimine. *Proc. Natl. Acad. Sci. U.S.A.* **1995**, *92*, 7297−7301. (b) Pichon, C.; Concalves, C.; Midoux, P. Histidine-rich peptides and polymers for nucleic acid delivery *Adv. Drug Delivery Rev.* **2001**, *53*, 75−94. (c) Kichler, A.; Leborgne, C.; März, J.; Danos, O.; Bechinger, B. Histidine-rich amphipathic peptide antibiotics promote efficient delivery of DNA into mammalian cells. *Proc. Natl. Acad. Sci. U.S.A.* **2003**, *100*, 1564−1568. (d) Thomas, M.; Klibanov, A. M. Enhancing polyethylenimine's delivery of plasmid DNA into mammalian cells. *Proc. Natl. Acad. Sci. U.S.A.* **2002**, *99*, 14640−14645.

10.1021/mp060045s CCC: $37.00
Published on Web 01/26/2007

as gene carriers. These organic−inorganic hybrid nanoparticles not only can be prepared easily but also overcome extra/intracellular barriers and exhibit higher transfection efficiency and drug transportation ability.[11] Klibanov et al. reported that branched polyethylenimine (PEI) modified gold nanoparticles enhance transfection efficiency 12 times compared to unmodified PEI.[10d] Davis and co-workers have demonstrated the use of cyclodextrin-containing polymers and/or cross-linked matrixes for DNA aggregation, serving as a highly tunable and biocompatible matrix for recombinant adenovirus-mediated gene delivery to local wound sites.[12] Recently, a new strategy of preparing biomaterials has been described in which functional systems have been constructed by noncovalent interactions, such as hydrophobic, electrostatic, hydrogen bonds, and van der Waals interactions. On the other hand, cyclodextrins (CDs), composed of six, seven, or eight D-glucopyranose units, possess truncated cone-shaped hydrophobic cavities which are capable of binding various organic,[13] inorganic,[14] and biological molecules to form stable host−guest inclusion complexes[15] or supramolecular aggregates.[16,17] Hence, they have been extensively used as supramolecular receptors in material science and biological technology. In the present work, we wish to report a novel CD-based DNA-binding receptor, i.e., oligo(ethylenediamino)-β-cyclodextrin-modified gold nanoparticle (OEA-CD-NP), that consisted of a gold nanoparticle as the core, oligo(ethylenediamino) chains attached to the primary side of the CD cavities as the electrostatic sites for binding DNA, and numerous CD cavities located at the external surface as a porous hydrophobic environment (Scheme 1). The aggregation behaviors of OEA-CD-NPs with DNA were investigated by several spectrophotometric and microscopic

(8) (a) Luo, D.; Saltzman, W. M. Enhancement of transfection by physical concentration of DNA at the cell surface. *Nat. Biotechnol.* **2000**, *18*, 893−895. (b) Tang, M. X.; Redemann, C. T.; Szoka, F. C. In vitro gene delivery by degraded polyamidoamine dendrimers. *Bioconjugate Chem.* **1996**, *7*, 703−714. (c) Radu, D. R.; Lai, C. Y.; Jeftinija, K.; Rowe, E. W.; Jeftinija, S.; Lin, V. S. Y. A polyamidoamine dendrimer-capped mesoporous silica nanosphere-based gene transfection reagent. *J. Am. Chem. Soc.* **2004**, *126*, 13216−13217.

(9) Kneuer, C.; Sameti, M.; Bakowsky, U.; Schiestel, T.; Schirra, H.; Schmidt, H.; Lehr, C. M. A nonviral DNA delivery system based on surface modified silica-nanoparticles can efficiently transfect cells in vitro. *Bioconjugate Chem.* **2000**, *11*, 926−932.

(10) (a) Niidome, T.; Nakashima, K.; Takahashi, H.; Niidome, Y. Preparation of primary amine-modified gold nanoparticles and their transfection ability into cultivated cells. *Chem. Commun.* **2004**, 1978−1979. (b) McIntosh, C. M.; Esposito, E. A.; Boal, A. K.; Simard, J. M.; Martin, C. T.; Rotello, V. R. Inhibition of DNA transcription using cationic mixed monolayer protected gold clusters. *J. Am. Chem. Soc.* **2001**, *123*, 7626−7629. (c) Sandhu, K. K.; McIntosh, C. M.; Simard, J. M.; Smith, S. W.; Rotello, V. M. Gold nanoparticle-mediated transfection of mammalian cells. *Bioconjugate Chem.* **2002**, *13*, 3−6. (d) Thomas, M.; Klibanov, A. M. Conjugation to gold nanoparticles enhances polyethylenimine's transfer of plasmid DNA into mammalian cells. *Proc. Natl. Acad. Sci. U.S.A.* **2003**, *100*, 9138−9143. (e) Liu, G.; Li, D.; Pasumarthy, M, K.; Kowalczyk, T. H.; Gedeon, C. R.; Hyatt, S. L.; Payne, J. M.; Miller, T. J.; Brunovskis, P.; Fink, T. L.; Muhammad, O.; Moen, R. C.; Hanson, R. W.; Cooper, M. J. Nanoparticles of compacted DNA transfect postmitotic cells. *J. Biol. Chem.* **2003**, *278*, 32578−32586.

(11) (a) Shenoy, D.; Little, S.; Langer, R.; Amiji, M. Poly(ethylene oxide)-modified poly(β-amino ester) nanoparticles as a pH-sensitive system for tumor-targeted delivery of hydrophobic drugs. 1. In vitro evaluations. *Mol. Pharmaceutics* **2005**, *2*, 357−366. (b) Sahoo, S. K.; Labhasetwar, V. Enhanced antiproliferative activity of transferrin-conjugated paclitaxel-loaded nanoparticles is mediated via sustained intracellular drug retention. *Mol. Pharmaceutics* **2005**, *2*, 373−383.

(12) Davis, M. E.; Pun, S. H.; Bellocq, N. C.; Reineke, T. M.; Popielarski, S. R.; Mishra, S.; Heidel, J. D. Self-assembling nucleic acid delivery vehicles via linear, water-soluble, cyclodextrin-containing polymers. *Curr. Med. Chem.* **2004**, *11*, 179−197.

(13) (a) Venema, F.; Nelissen, H. F. M.; Berthault, P.; Birlirakis, N.; Rowan, A. E.; Feiters, M. C.; Nolte, R. J. M. Synthesis, conformation, and binding properties of cyclodextrin homo- and heterodimers connected through their secondary sides. *Chem. Eur. J.* **1998**, *4*, 2237−2250. (b) Kano, K.; Nishiyabu, R.; Asada, T.; Kuroda, Y. Static and dynamic behavior of 2:1 inclusion complexes of cyclodextrins and charged porphyrins in aqueous organic media. *J. Am. Chem. Soc.* **2002**, *124*, 9937−9944. (c) Mayer, B.; Zhang, X.; Nau, W. M.; Marconi, G. Co-conformational variability of cyclodextrin complexes studied by induced circular dichroism of azoalkanes. *J. Am. Chem. Soc.* **2001**, *123*, 5240−5248.

(14) Szejtli, J.; Osa, T. *Comprehensive Supramolecular Chemistry, Volume 3: Cyclodextrins*; Pergamon Press: Oxford, U.K., 1996.

(15) (a) Connors, K. A. The stability of cyclodextrin complexes in solution. *Chem. Rev.* **1997**, *97*, 1325−1358. (b) Huskens, J.; Deij, M. A.; Reinhoudt, D. N. Writing patterns of molecules on molecular printboards, *Angew. Chem., Int. Ed.* **2002**, *41*, 4467−4471.

(16) (a) Dvornikovs, V.; House, B. E.; Kaetzel, M.; Dedman, J. R.; Smithrud, D. B. Host-[2]-rotaxanes as cellular transport agents. *J. Am. Chem. Soc.* **2003**, *125*, 8290−8301. **(**b) Kidd, T. J.; Loontjens, T. J. A.; Leigh, D. A.; Wong, J. K. Y. Rotaxane building blocks bearing blocked isocyanate stoppers: polyrotaxanes through post-assembly chain extension. *Angew. Chem., Int. Ed.* **2003**, *42*, 3379−3383. (c) Long, B.; Nikitin, K.; Fitzmaurice, D. Self-assembly of a tripodal pseudorotaxane on the surface of a titanium dioxide nanoparticle. *J. Am. Chem. Soc.* **2003**, *125*, 5152−5160. (d) Pease, A. R.; Jeppesen, J. O.; Stoddart, J. F.; Luo, Y.; Collier, C. P.; Heath, J. Switching devices based on interlocked molecules. *Acc. Chem. Res.* **2001**, *34*, 433−444. (e) Ohira, A.; Sakata, M.; Taniguchi, I.; Hirayama, C.; Kunitake, M. Comparison of nanotube structures constructed from α, β and γ-cyclodextrins by potential-controlled adsorption. *J. Am. Chem. Soc.* **2003**, *125*, 5057−5065. (f) Miyake, K.; Yasuda, S.; Harada, A. Sumaoka, J.; Komiyama, M.; Shigekawa, H. Formation process of cyclodextrin necklace-analysis of hydrogen bonding on a molecular level. *J. Am. Chem. Soc.* **2003**, *125*, 5080−5085. (g) Yamashita, A.; Choi, H. S.; Ooya, T.; Yui, N.; Akita, H.; Kogure, K.; Harashima, H. Improved cell viability of linear polyethylenimine through γ-cyclodextrin inclusion for effective gene delivery. *ChemBioChem* **2006**, *7*, 297−302.

(17) (a) Liu, Y.; Wang, H.; Chen, Y.; Ke, C. F.; Liu, M. Supramolecular aggregates constructed from gold nanoparticles and L-Try-CD polypseudorotaxanes as captors for fullerenes. *J. Am. Chem. Soc.* **2005**, *127*, 657−666. (b) Liu, Y.; Wang, H.; Liang, P.; Zhang, H. Y. Water-soluble supramolecular fullerene assembly mediated by metallobridged β-cyclodextrins. *Angew. Chem., Int. Ed.* **2004**, *43*, 2690−2694.

Scheme 1

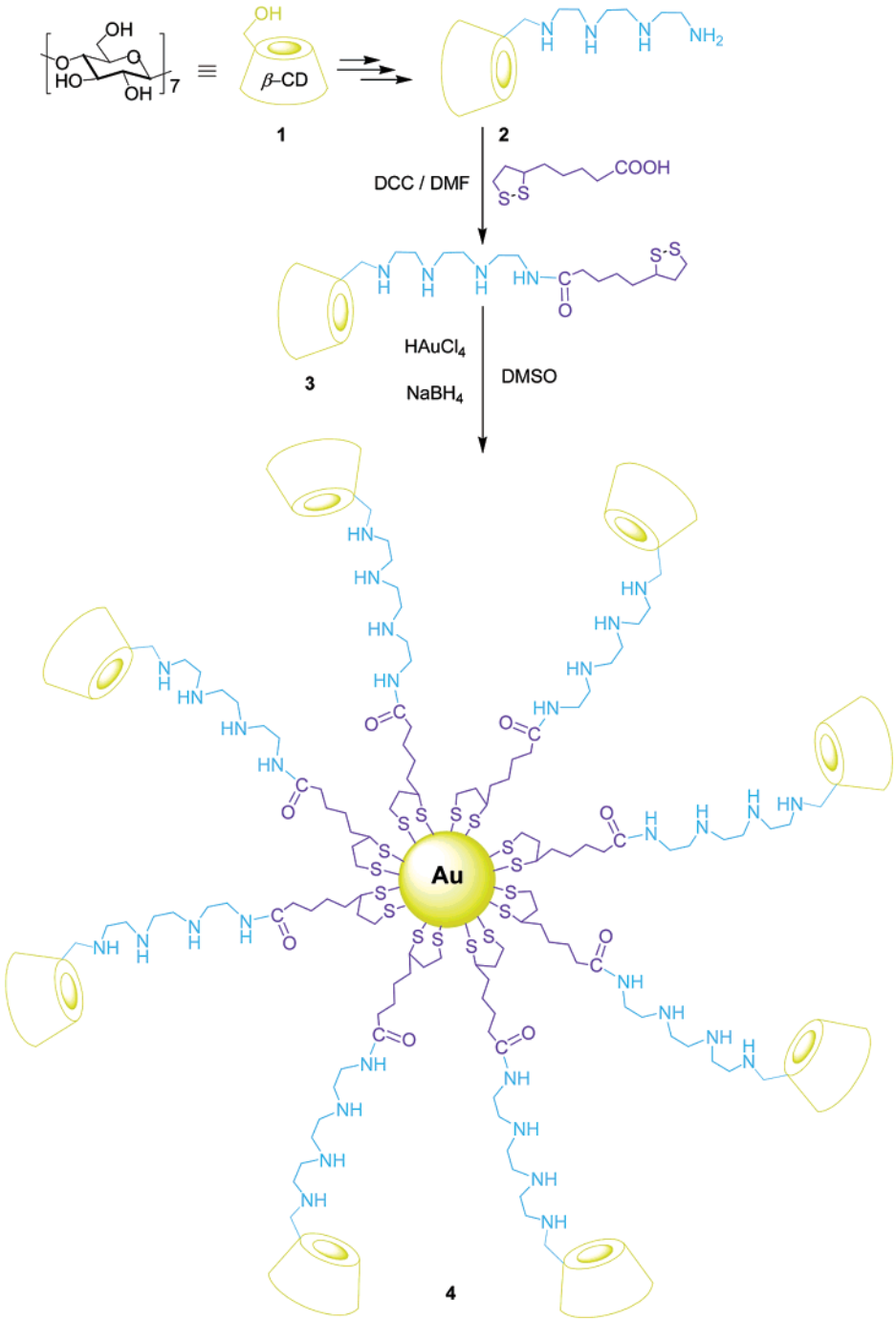

techniques, which indicated that the formation and morphological structure of aggregate directly depended on initial quantity of OEA-CD-NP receptor and DNA. Furthermore, the gene delivery experiments *in vitro* demonstrated that this DNA receptor successfully delivered the pEGFPC1 plasmid DNA into human breast cancer MCF-7 cell line (MCF-7).

Experimental Section

General. All solvents and reagents were purchased from commercial sources and used as received unless otherwise noted. β-CD was recrystallized twice from water and vacuum-dried before use. Mono(6-triethylenetetraamino-6-deoxy)-β-CD (**2**) was prepared according to a literature method.[18] NMR spectra were recorded on a Varian INVOA 300 spectrometer in D_2O. FT-IR spectra were recorded on a Shimadzu Bio-Rad FTS 135 instrument. UV−vis spectra were recorded in a conventional quartz cell (10 × 10 × 45 mm) at 25 °C on a Shimadzu UV2401 spectrometer. The ICP experiment was performed on an ICP-9000 (N + M) instrument (U.S.A. Thermo Jarrell-Ash Corporation). Deion-

(18) Petter, R. C.; Salek, J. S.; Sikorski, C. T.; Kumaravel, G.; Lin, F.-T. Cooperative binding by aggregated mono-6-(alkylamino)-β-cyclodextrins. *J. Am. Chem. Soc.* **1990**, *112*, 3860−3868.

ized, triple distilled water was used as solvent in all spectral and biological activity measurements.

Absorption and Circular Dichroism Spectroscopy. Each sample for absorption and CD spectroscopic measurements was prepared by adding the required volume of a phosphate buffer solution (pH 7.20) of OEA-CD-NP to a phosphate buffer solution (pH 7.20) of calf thymus DNA (HuaMei Chemical Company). The DNA concentration was determined by measuring the UV absorbance at 260 nm (ϵ = 6600 M^{-1} cm^{-1}). Typically, the DNA concentration was ca. 30 μg/mL (ca. 50 μM) in base pairs.[19] The stock solution of DNA was stored at 4 °C and kept at room temperature for 1 h before use. The w/w ratio between OEA-CD-NP and DNA was varied according to the experimental procedure.

Transmission Electron Microscopic (TEM) Measurements. A 50 μL portion of sample solution was dropped on a copper grid. The grid was then air-dried. The samples were examined by a high-resolution transmission electron microscope (TEM) (Philips Tecnai G^2 20 S-TWIN microscope) operating at an accelerating voltage of 200 keV.

Synthesis of Modified β-CD 3. To a solution of DMF (30 mL) containing lipoic acid (0.4 g) and dicyclohexylcarbodiimide (DCC) (0.3 g) was added 1.3 g of mono(6-triethylenetetraamino-6-deoxy)-β-CD (**2**). The resultant mixture was stirred for 2 days in an ice bath and another 3 days at room temperature until no more precipitation deposited. The precipitate was removed by filtration, and the filtrate was evaporated to dryness under reduced pressure. The residue was dissolved in a minimum amount of hot water and then poured into 300 mL of acetone. The precipitate formed was collected by filtration to obtain a white powder, which was purified on a column of Sephadex G-25 to give 0.5 g (34% yield) of **3** as a light yellow solid: ESI-MS *m*/*z* observed 1469.7 ($M + NH_4^+$); ^{1}H NMR (D_2O) δ 1.19−1.82 (m, 8H), 2.01−3.16 (m, 19H), 3.35−3.83 (m, 42H), 4.95−5.01 (m, 7H); FT-IR (KBr) ν 3333, 2921, 1651, 1558, 1455, 1333, 1154, 1078, 1032, 943 cm^{-1}. Anal. Calcd for $C_{56}H_{98}O_{35}N_4S_2 \cdot 6H_2O$: C, 43.13; H, 7.11; N, 3.59. Found: C, 43.44; H, 7.43; N, 3.78.

Synthesis of OEA-CD-NP 4. $HAuCl_4 \cdot 4H_2O$ (50 mg) was dissolved in 20 mL of DMSO. This solution was quickly mixed with another 20 mL of DMSO containing 75.5 mg of $NaBH_4$ and 20 mg of **3**, and the reaction mixture turned deep brown immediately. After the reaction mixture was stirred for 24 h at room temperature, 40 mL of CH_3CN was added to give a black precipitate. The product was collected by centrifugation, washed two times with 60 mL of CH_3CN: DMSO (v:v = 1:1) and 60 mL of ethanol, and dried under vacuum for 12 h at 80 °C: ^{1}H NMR (D_2O) δ 1.19−1.82 (m, 8H), 2.01−3.16 (m, 19H), 3.35−3.83 (m, 42H), 4.95−5.01 (m, 7H); FT-IR (KBr) ν 3353, 2910, 1652, 1559, 1433, 1340, 1157, 1033 cm^{-1}. Experimental elemental analysis data (%): C, 14.49; H, 4.29; N, 0.92. ICP (%): Au, 33.90.

Synthesis of 5. A solution of chloroform (10 mL) containing lipoic acid (1.05 g) was added slowly to a solution of chloroform (20 mL) containing triethylenetetraamine (1.5 mL) and dicyclohexylcarbodiimide (DCC, 1.1 g) (Scheme 2). The resultant mixture was stirred for 1 day in an ice bath and another 3 days at room temperature until no more precipitation deposited. The precipitate was removed by filtration, and the filtrate was evaporated to dryness under reduced pressure. The residue was dissolved in a minimum amount of ethyl acetate and purified by column chromatography using silica gel to give 0.95 g (56% yield) of **5** as a light yellow solid: ESI-MS *m*/*z* observed 335.5 ($M + H^+$); ^{1}H NMR ($CDCl_3$) δ 1.32−1.81 (m, 6H), 1.92 (m, 2H), 2.35−2.54 (m, 14H), 3.13 (m, 2H), 3.57 (m, 1H). Anal. Calcd for $C_{14}H_{30}ON_4S_2$: C, 50.26; H, 9.04; N, 16.75. Found: C, 50.42; H, 8.83; N, 16.65.

Synthesis of OEA-L-NP 6. $HAuCl_4 \cdot 4H_2O$ (50 mg) was dissolved in 20 mL of DMSO. This solution was quickly mixed with another 20 mL of DMSO containing 75.5 mg of $NaBH_4$ and 5 mg of **5**, and the reaction mixture turned deep brown immediately. After the reaction mixture was stirred for 24 h at room temperature, 40 mL of CH_3CN was added to give a black precipitate. The product was collected by centrifugation, washed two times with 60 mL of CH_3CN: DMSO (v:v = 1:1) and 60 mL of ethanol, and dried under vacuum for 12 h at 80 °C to give **6**: ^{1}H NMR (D_2O) δ 1.18−1.82 (m, 8H), 2.14−3.10(m, 17H). Experimental elemental analysis data (%): C, 5.36; H, 1.68; N, 1.65. ICP (%): Au, 58.27.

Characterization of OEA-CD-NP. By assuming the core shape of nanoparticles to be spherical, the average number of CD units around one nanoparticle (N) and the average surface area occupied by one CD unit (Ψ) could be calculated by the equations listed below:

$$M_{\text{Au-NPs}} = \frac{W_{\text{Au}}}{D_{\text{Au}}(4/3)\pi r^3 N_{\text{A}}} \quad (1)$$

$$M_{\text{CD}} = \frac{W_{\text{CD}}}{\text{MW}_{\text{CD}}} \quad (2)$$

$$N = \frac{M_{\text{CD}}}{M_{\text{Au-NPs}}} = \frac{W_{\text{Au}}\text{MW}_{\text{CD}}}{W_{\text{CD}}D_{\text{Au}}(4/3)\pi r^3 N_{\text{A}}} \quad (3)$$

$$\Psi = \frac{S_{\text{Au}}}{N} \quad (4)$$

where $M_{\text{Au-NP}}$ and M_{CD} are the molar number of gold nanoparticles and **3**, respectively. W_{Au}, W_{CD}, and D_{Au} are the gold content, cyclodextrin content, and gold density, respectively. r is the radius of nanoparticles. N_{A} is the Avogadro constant (6.02×10^{23}). MW_{CD} is the molecular weight of **3**. S_{Au} is the surface area of the Au-NPs. N is the number of **3** on each of nanoparticles, and Ψ is the average surface area occupied by one CD unit.

From eqs 3 and 4, it could be calculated that the average number of CD units around one nanoparticle is 37 according to the elemental analysis and ICP data, and the average surface area occupied by one CD unit is 1.64 nm^2.

(19) Ottaviani, M. F.; Furini, F.; Casini, A.; Turro, N. J.; Jockusch, S.; Tomalia, D. A.; Messori, L. Formation of supramolecular structures between dna and starburst dendrimers studied by EPR, CD, UV, and melting profiles. *Macromolecules* **2000**, *33*, 7842−7851.

Scheme 2

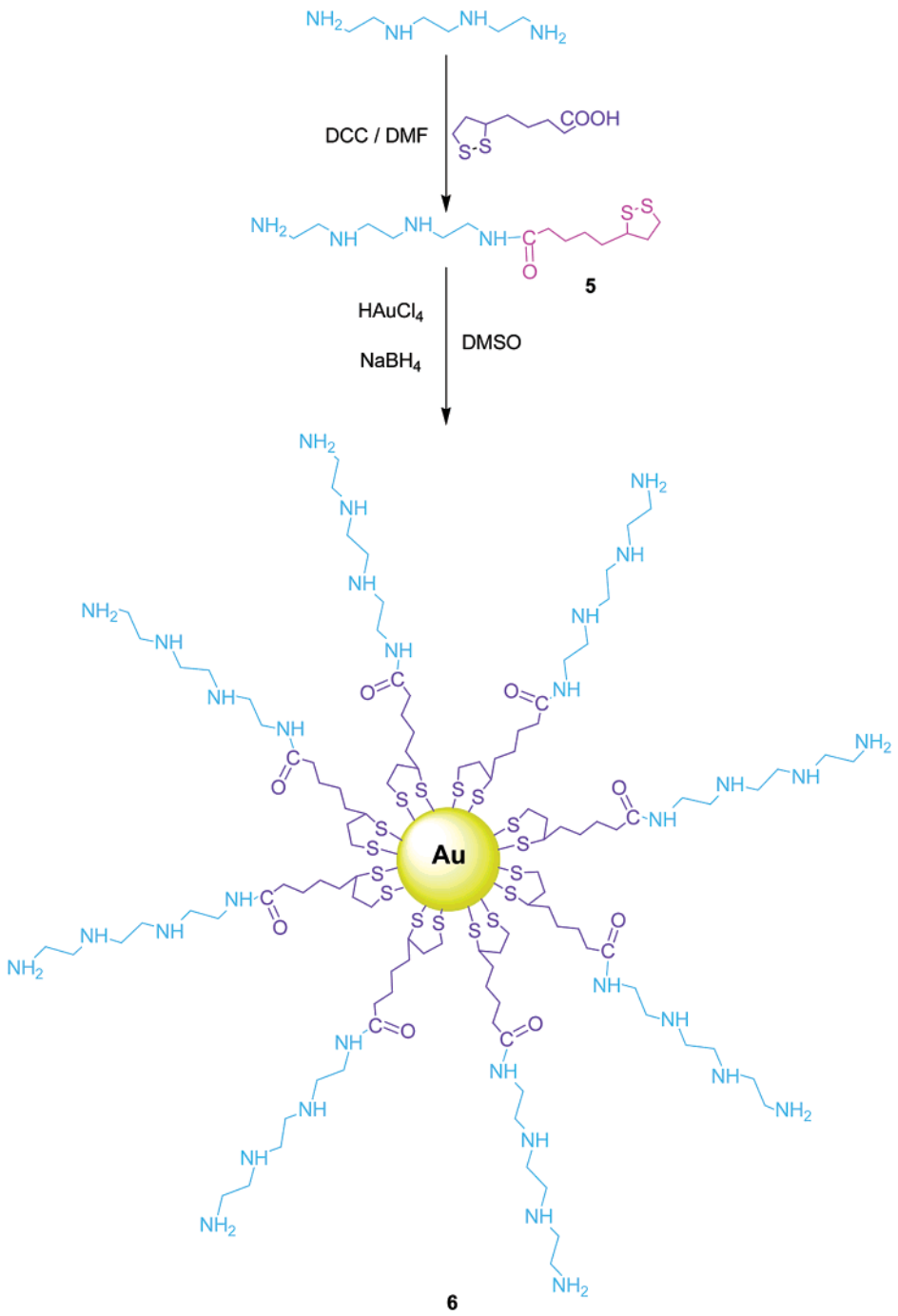

DNA Plasmid. pEGFPC1 (4.7 kb) was provided by the State Key Laboratory of Experimental Hematology (China). This plasmid was obtained as a 1.0 mg/mL stock solution in aqueous Tris-HCl/EDTA buffer (pH 7.0).

Preparation of OEA-CD-NP/DNA Aggregates. OEA-CD-NP (16.8 mg) was dissolved in 1 mL of water as a stock solution, which was sterilized and stored at 4 °C. Before reacting with DNA, the stock solution of OEA-CD-NPs was brought to room temperature and diluted with water. OEA-CD-NP/DNA aggregates were prepared by adding a water solution (50 μL) containing an appropriate amount of OEA-CD-NP to a mixture composed of 25 μL of water containing 0.8 μg of plasmid DNA and 25 μL of 2XHBS[20] buffer solution, and incubating the resultant solution at 37 °C for 20 min.

Cell Culture and Transfection. The human breast cancer MCF-7 cell line (MCF-7) was obtained from the State Key Laboratory of Experimental Hematology. Cells were maintained in RPMI 1640 medium containing 10% FCS and cultured in a humidified, 5% CO_2 atmosphere tissue culture

(20) The 2XHBS buffer was prepared by 50 mM HEPES, 10 mM KCl, 280 mM NaCl, 1.5 mM Na_2HPO_4, and 12 mM dextrose and careful adjustment of the pH value to 7.0.

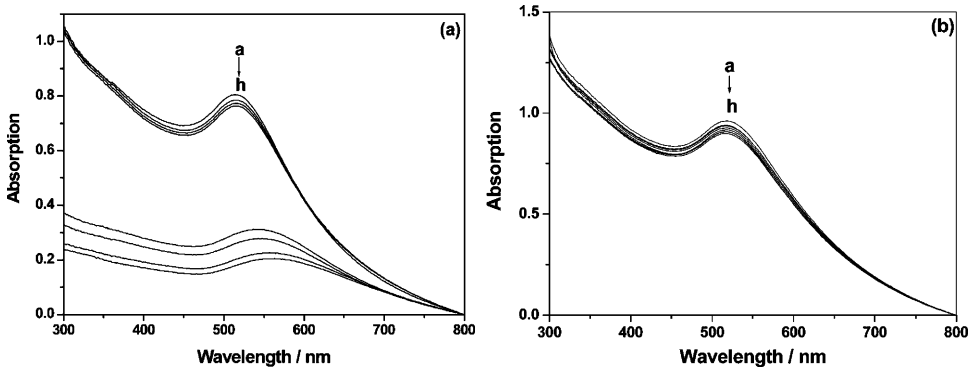

Figure 1. The SPR band changes of (a) OEA-CD-NP and (b) OEA-L-NP with a fixed concentration of 0.3 mg mL^{-1} upon addition of ct-DNA in pH 7.2 phosphate buffer ($M = 0.1$). The w/w ratios of the ct-DNA and OEA-CD-NP or OEA-L-NP were 0, 1, 0.67, 0.33, 0.2, 0.1, 0.02, 0.01 from a to h, respectively.

incubator. In the experiment, cells (5×10^4 per well) were plated on 24-well tissue-culture clusters for 24 h before transfection and digested with 0.25% steapsin containing 0.01% EDTA. The digestion process was stopped by addition of RPMI 1640 with 10% FCS. Before the initiation of transfection experiments, the medium was removed from each well, and cells were washed once with RPMI 1640 without serum and antibiotics. To each well, 100 μL of OEA-CD-NP/DNA transfection medium was added with shaking, followed by incubation at 37 °C in a humidified-air (5% CO_2) atmosphere for 8 h. Then, the transfection medium was removed, and cells were washed with D-Hanks. After adding RPMI 1640 containing 10% FCS medium, cells were further incubated under the same conditions in a complete medium for 48 h. The nuclear staining experiments showed that above 90% cells were still alive. As a safe estimation, 95% cells are viewed as alive after the incubation process. Then, 500 cell samples were monitored by fluorescent microscopy, and the transfection efficiency was calculated using a statistical method because of the transfected cells emitting green fluorescence different from the living cells.

Cytotoxicity Experiments. Cell culture was performed under the same conditions as outlined above. Control cells were treated with RPMI 1640 containing 25 μL of 2XHBS, whereas other cells were treated with either lipofectamine 2000 or OEA-CD-NP/DNA aggregates. Cytotoxicity measurements were performed as follows: In each well, 0.5 mL of MCF-7 cells, 0.1 mL of 0.4% trypan blue, and the assayed transfection mediums were mixed together, and the resulting solution was kept for 2 min at 37 °C. Then, 200 cell samples were checked by microscopy, where dead cells turned blue but living ones remained unchanged, to calculate the percentages relative to control cells.

Results and Discussion

Electronic Absorption Spectra. To investigate the aggregation behaviors of OEA-CD-NP with DNA in solution, the electronic absorption spectra of OEA-CD-NP in the presence of calf thymus DNA (ct-DNA) in varying concentrations were recorded (Figure 1a). Since the absorption maximum of OEA-CD-NP at 260 nm overlapped with that of the ct-DNA, we only analyzed the absorption maximum of OEA-CD-NP beyond 520 nm, which is assigned to the surface plasmon resonance (SPR) band of gold nanoparticle. Generally, the aggregation of gold nanoparticles leads to the appearance of a new absorption band at a longer wavelength than that of the discrete gold nanoparticles as a result of the electric dipole−dipole interactions and the coupling between the plasmons of neighboring particles in the formed aggregates.[21] Similar phenomena were also found in our experiments. As can be seen from Figure 1a, the original SPR maximum of OEA-CD-NP at 515 nm decreased with the gradual addition of ct-DNA. A further examination showed that, when the ratio (w/w) between OEA-CD-NP and ct-DNA was relatively lower (lines b−d), the intensity of OEA-CD-NP's SPR band slightly decreased with the addition of ct-DNA, but the absorption maximum did not shift. However, when this ratio increased to a moderate proportion (lines e and f), the intensity of absorption maximum of OEA-CD-NP's SPR band remarkably decreased by 65.5%, accompanied by an obvious bathochromic shift of the SPR maximum from 515 to 544 nm. Simultaneously, the color of the solution changed from red to blue-violet. These phenomena jointly indicated an effective aggregation of OEA-CD-NPs. Keeping on increasing the ratio (w/w) between OEA-CD-NP and ct-DNA to a larger proportion (lines g and h), the intensity of OEA-CD-NP's SPR band further decreased, accompanied by bathochromic shifts of the SPR absorption maximum, but the decline tendency turned smooth. These results demonstrated a high OEA-CD-NP/DNA ratio in favor of formation of larger aggregates, and meanwhile the distance of particles from each other decreased, which would directly result in conformational changes and concentration of DNA. For comparative purposes, the electronic absorption spectra of OEA-L-NP in the presence of calf thymus DNA (ct-DNA) in varying concentrations were also recorded (Figure 1b). The main parameters (λ_{max} and ϵ) of the UV absorption band of OEA-L-NP were almost unchanged upon the gradual addition of DNA. It is

(21) Storhoff, J. J.; Lazarides, A. A.; Mucic, R. C.; Mirkin, C. A.; Letsinger, R. L.; Schatz, G. C. What controls the optical properties of DNA-linked gold nanoparticle assemblies? *J. Am. Chem. Soc.* **2000**, *122*, 4640−4650.

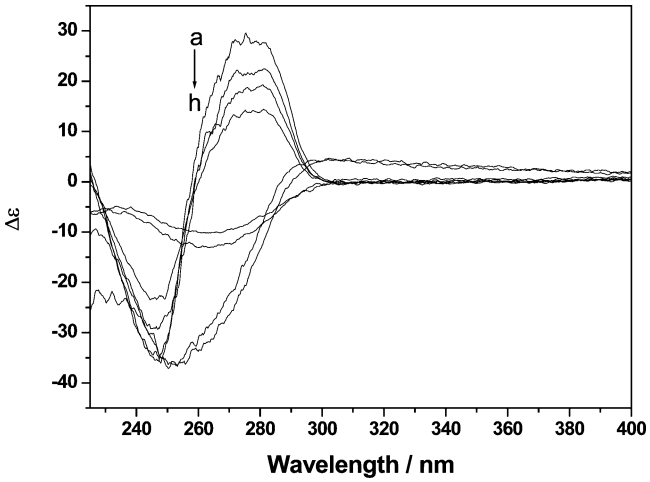

Figure 2. The circular dichroism spectra of ct-DNA (0.15 mg mL^{-1}) upon addition of OEA-CD-NP in pH 7.2 phosphate buffer (0.1 M). The concentration of OEA-CD-NP was 0, 0.2, 0.5, 0.8, 3.0, 6.0, 12.0, 24.0 mg mL^{-1} from a to h. Cell length: 1 cm.

supposed that no significant aggregate is formed between OEA-L-NP and DNA. This phenomenon can further confirm the crucial factor of cyclodextrin in the aggregation of OEA-CD-NP with DNA.

Circular Dichroism Spectra. Because the UV−vis spectrum of ct-DNA overlapped with that of OEA-CD-NP around 260 nm, we employed circular dichroism spectroscopy, which is undoubtedly one of the most useful techniques for investigating the solution structure of DNA and the conformational twist of the double helix produced by the formation of supramolecular aggregates, to study the possible structural change of DNA upon associated with OEA-CD-NP. Figure 2 illustrates circular dichroism spectra of ct-DNA with the gradual addition of OEA-CD-NP. The intrinsic circular dichroism activity of OEA-CD-NP was recorded and found to be negligible. The observed effects on the circular dichroism spectra produced by gradual addition of increasing amount of OEA-CD-NP are shown in Figure 2. At low OEA-CD-NP/DNA ratio (lines a−d), only minor effects on the B-type circular dichroism spectrum of calf thymus DNA were detected; more precisely, the addition of OEA-CD-NP produced a modest decrease of the positive band at 275 nm and of the negative band at 245 nm. Notably, when the OEA-CD-NP/DNA ratio reached a moderate value (lines e and f), the circular dichroism signal of DNA was obviously changed and only a relatively weaker negative Cotton effect peak at 260 nm was observed as a result of modest aggregate of DNA. However, by further increasing the OEA-CD-NP/DNA ratio (lines g and h), the negative Cotton effect peak was enhanced and blue-shifted from 260 to 250 nm, indicating that extensive condensation of DNA had happened. The results that the circular dichroism spectra were also not changed significantly by the gradual addition of increasing amount of OEA-L-NP to ct-DNA (see the Supporting Information) demonstrated that the solution structure of ct-DNA was immobile by the addition of OEA-L-NP.

Transition Electronic Microscopy (TEM). Direct information about the shape, size, and distribution of OEA-CD-NP/DNA aggregates came from TEM results. Under our experimental conditions, the average gold core size of gold nanoparticles was 4.3 ± 0.7 nm (based on individual measurements on at least 140 particles) (Figure 3A). When the ct-DNA was added, OEA-CD-NP tended to aggregate, but the aggregation behavior was found to be strongly dependent on the initial ratio (w/w) between OEA-CD-NP and DNA. For example, when the initial ratio ($w_{OEA-CD-NP}/w_{DNA}$) was 0.1:1, no appreciable aggregation of gold nanoparticles was observed, and OEA-CD-NP still existed as discrete particles (Figure 3B). A possible reason for this phenomenon was that, in the presence of a large amount of DNA, every gold nanoparticle was surrounded by one or several DNA chains, which blocked the contact between particles and thus restrained the aggregation. When $w_{OEA-CD-NP}/w_{DNA}$ was increased to 5:1, obvious aggregation of OEA-CD-NP was observed (Figure 3C). In order to recognize their specific structural information, an amplified picture of Figure 3C is shown in Figure 3D, in which the DNA twisted segments were surface-coated by OEA-CD-NP. At this concentration ratio, nearly all OEA-CD-NPs were adsorbed on DNA segments. UV spectroscopy showed that the SPR absorption of OEA-CD-NP was decreased compared with naked OEA-CD-NP, which was demonstrated in the previous section. Further increasing the $w_{OEA-CD-NP}/w_{DNA}$ ratio to 100:1 resulted in highly compacted OEA-CD-NP/DNA aggregates (Figure 3E,F) with an average diameter larger than 100 nm. These results were identical with the conclusion drawn from UV−vis results, that is, a high $w_{OEA-CD-NP}/w_{DNA}$ ratio would promote the aggregation of OEA-CD-NP. It should be noted that there also existed some linear structures (marked with blue arrows) in TEM images, assigned to self-aggregated DNAs. Therefore, we deduced that there should exist a competition in solution between the OEA-CD-NP/DNA aggregation and the self-aggregation of DNA. At a high $w_{OEA-CD-NP}/w_{DNA}$ ratio, OEA-CD-NP/DNA aggregation may predominate. TEM results also confirmed no appreciable aggregation of OEA-L-NP by addition of ct-DNA (Figure 4), which is consistent with the results of UV−vis and CD experiments.

Transfection Assay of OEA-CD-NP/*p*-DNA Aggregates. The transfection efficiency of the OEA-CD-NP/DNA aggregate *in vitro* into MCF-7 cells was tested with the plasmid DNA, which contains a recombinant adenovirus encoding GFP. The visual GFP expression results were corroborated when the plates were quantitatively analyzed with a fluorometer. Fluorescent pictures of visible GFP expression (Figure 5) suggested that OEA-CD-NP was able to act as a gene vector to transfer the GFP information into cells. When OEA-CD-NP/*p*-DNA aggregates at various w/w ratios were added to MCF-7 cells, significant gene expression was observed and its level was dependent on the w/w ratio between OEA-CD-NP and DNA. At incubation for 48 h, the percent of GFP-expressed cells was calculated by a statistical method and the transfection efficiency was defined

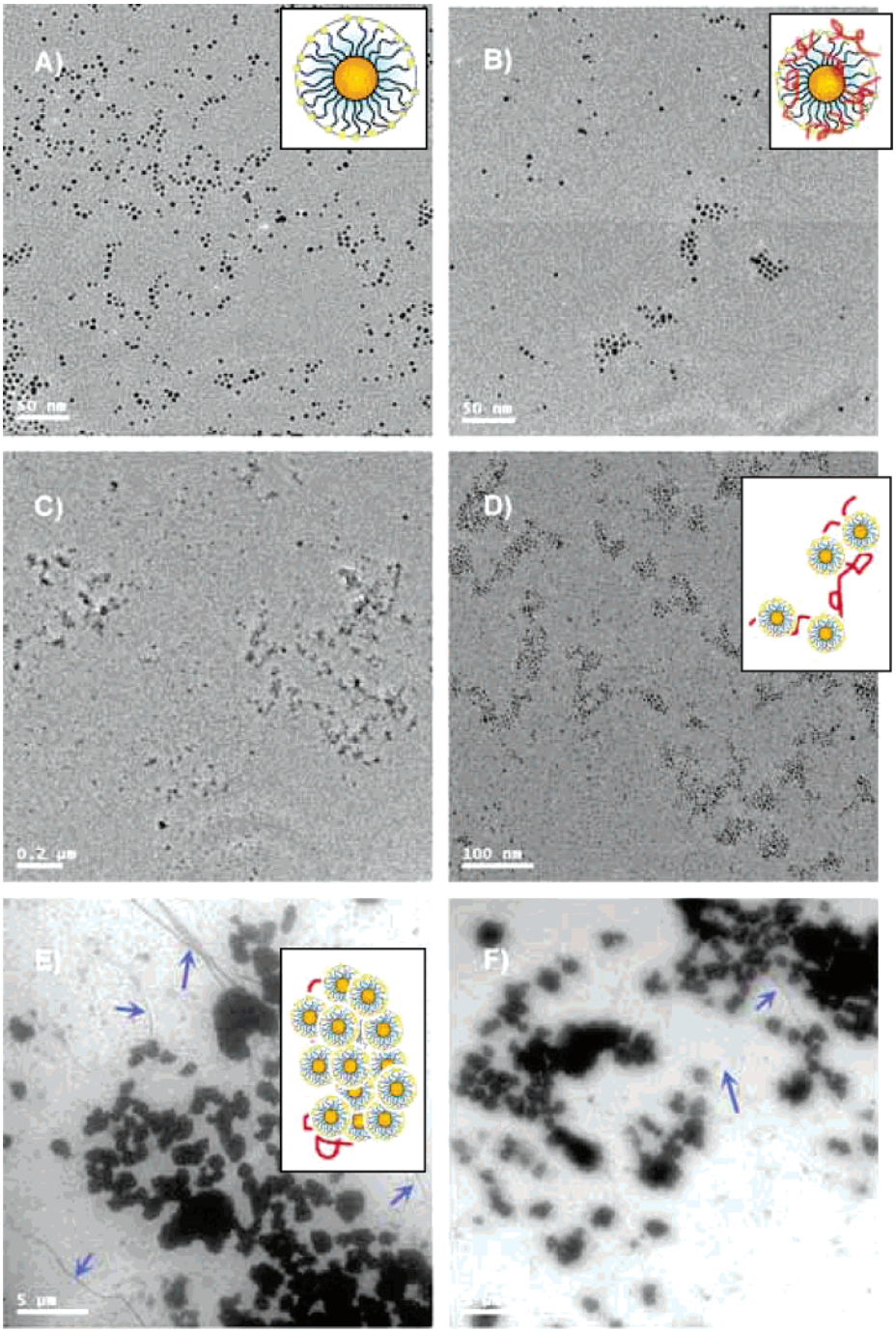

Figure 3. TEM images (A) OEA-CD-NP; (B) OEA-CD-NP/DNA mixture with a $w_{OEA-CD-NP}/w_{DNA}$ ratio of 0.1:1; (C) OEA-CD-NP/DNA mixture with a $w_{OEA-CD-NP}/w_{DNA}$ ratio of 5:1; (D) enlarged high-resolution TEM image of C; (E, F) OEA-CD-NP/DNA mixture with a $w_{OEA-CD-NP}/w_{DNA}$ ratio of 100:1.

as the percent of expressed cells in all examined living cells. In typical experiments, OEA-CD-NP/*p*-DNA aggregates with $w_{OEA-CD-NP}/w_{DNA}$ ratios (from 20 to 400) were tested, and corresponding transfection efficiencies are shown in Figure 6. As can be seen from Figure 6, OEA-CD-NP/*p*-DNA aggregates displayed moderate transfection efficiencies (from 1.2% to 4.8%) as compared with lipofectamine 2000 ($w_{lipo-2000}/w_{DNA}$ ratios 2:1), a widely used commercially available transfection agent. Although the artificial virus **4** suffered from low efficiencies compared with that of lipofectamine 2000, improvements may be achieved by the chemical modification of carriers or the optimization of mixed ratio between carriers and DNA.[22] In control experiments, natural β-CD **1** and modified β-CDs **2** and **3** did not show any transfection effects under the same conditions.

(22) Diebold, S. S.; Lehrmann, H.; Kursa, M.; Wagner, E.; Cotton, M.; Zenke, M. Efficient gene delivery into human dendritic cells by adenovirus polyethylenimine and mannose polyethylenimine transfection. *Hum. Gene Ther.* **1999**, *10*, 775−786.

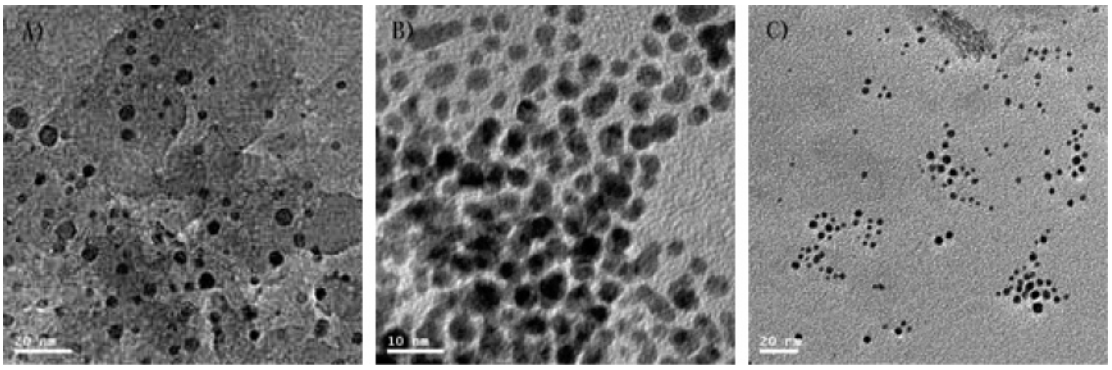

Figure 4. TEM images (A) OEA-L-NP; (B) OEA-L-NP/DNA mixture with a $w_{OEA-L-NP}/w_{DNA}$ ratio of 5:1; (C) OEA-L-NP/DNA mixture with a $w_{OEA-L-NP}/w_{DNA}$ ratio of 100:1.

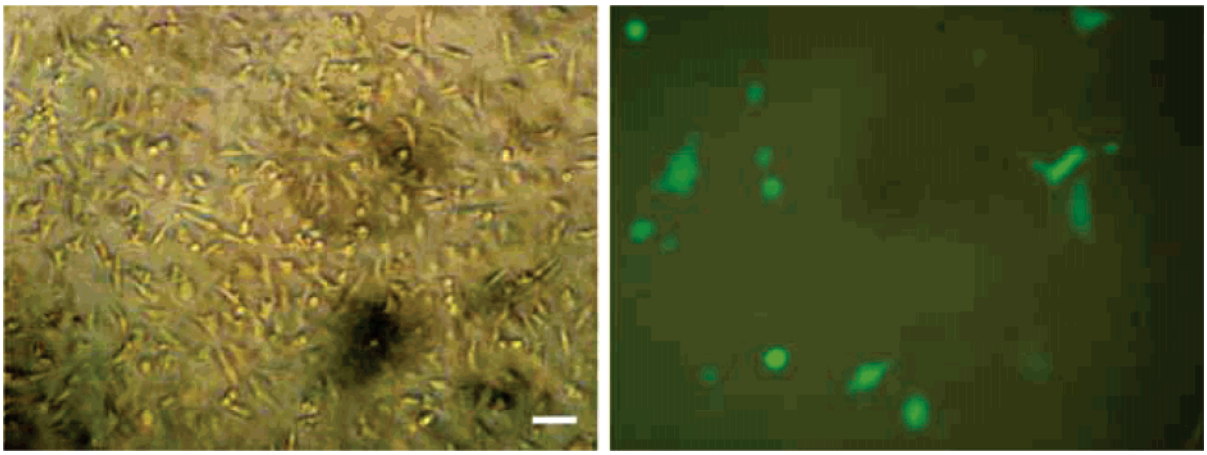

Figure 5. *In vitro* transduction of MCF-7 cells with OEA-CD-NP/*p*-DNA aggregate ($w_{OEA-CD-NP}/w_{DNA}$ ratio = 160): left photo, phase contrast; right photo, fluorescence. Scale bar: 20 μm.

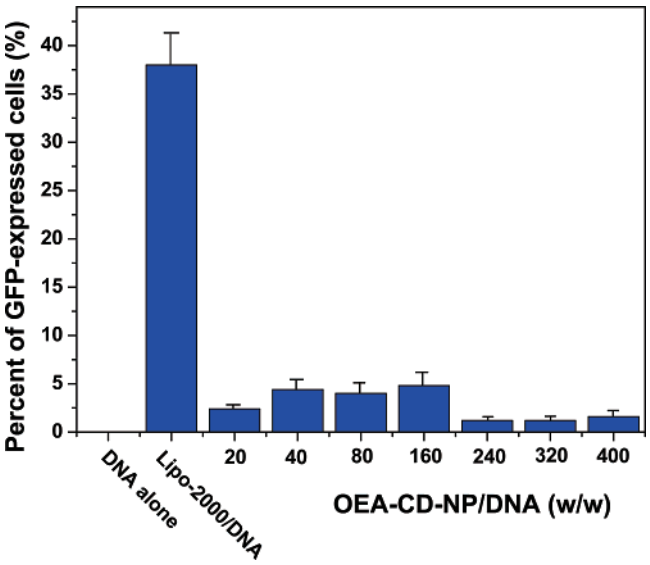

Figure 6. Percent of GFP-expressed MCF-7 cells with different $w_{OEA-CD-NP}/w_{DNA}$ ratios in RPMI 1640 containing 10% FCS medium.

Cytotoxicity Assay. Cytotoxicity assay results of OEA-CD-NP/DNA aggregates with different $w_{OEA-CD-NP}/w_{DNA}$ ratios are presented in Table 1. We can see that OEA-CD-NP/DNA aggregates exhibited lower cytotoxicities than lipofectamine 2000/DNA. For example, more than 96% of cells were still alive in the presence of OEA-CD-NP/DNA aggregates, whereas this percentage decreased to 94.5% in the case of lipofectamine 2000/DNA. The small cytotoxicity of OEA-CD-NP probably arose from the extrusive CD cavities on the surface of OEA-CD-NP/DNA aggregate protecting the plasma membranes of cells from deposition

Table 1. Cytotoxicities of OEA-CD-NP/*p*-DNA Aggregates to MCF-7 Cells[a]

gene carriers:	none	lipo-2000	OEA-CD-NP/DNA (w/w) 20	40	80	160	240	320	400
cell viability (%)	100	94.5	99.5	98.5	98.5	98.0	97.5	96.5	96.0

[a] Cytotoxicity was measured by the trypan blue assay. The viability of nontransfected cells alone was taken as 100%.

(23) (a) Fischer, D.; Bieber, T.; Li, Y.; Elsasser, H.-P.; Kissel, T. A novel non-viral vector for DANN delivery based on low molecular weight, branched polyethylenimine: effect of molecular weight on transfection efficiency and cytotoxicity. *Pharm. Res.* **1999**, *16*, 1273−1279. (b) Bieber, T.; Meissner, W.; Kostin, S.; Niemann, A.; Elsasser, H.-P. Intracellular route and transcriptional competence of polyethylenimine-DNA complexes. *J. Controlled Release* **2002**, *82*, 441−454.

by gold clusters, because a number of investigations revealed that the exposed gold clusters might impair the plasma-membrane functions and lead to cell death.[23]

Acknowledgment. We thank the National Natural Science Foundation of China (90306009, 20402008, 20421202, and 20572052), 973 Program (2006CB932900), and Tianjin Natural Science Foundation (06YFJMJC04400) for financial support.

Supporting Information Available: The circular dichroism spectra for the interaction of OEA-L-NP with DNA. This material is available free of charge via the Internet at http://pubs.acs.org.

MP060045S